IJMS 2021 8(1) 114 - 124

International Journal of Multidisciplinary Studies (IJMS)
Volume 8, Issue 1, 2021

Optimization of the absorber layer thicknesses and the surface defect densities of CdTe/Si tandem device.

Ratnasinghe D.R.[1], Attygalle M.L.C.[2*] and Mahabaduge H.P.[3]

[1]Faculty of Graduate Studies, University of Sri Jayewardenepura, Gangodawila, Nugegoda Sri Lanka
[2]Department of Physics, Faculty of Applied Sciences, University of Sri Jayewardenepura, Gangodawila, Nugegoda, Sri Lanka
[3]Department of Chemistry, Physics and Astronomy, Georgia College & State University, Milledgeville, GA 31061, USA

ABSTRACT

In this research, the performance variation of a newly modeled tandem device was investigated. A thin-film photovoltaic tandem device was created with a CdS/CdTe top cell configuration and a thick Si bottom cell configuration. The goal of this numerical simulation study was to enhance the performance of the tandem photovoltaic device. Therefore several modifications and optimizations were done to the device structure. An Mg-doped ZnO-based (MZO) layer was used as a High Resistance Transparent (HRT) layer with a very thin CdS layer. The thickness of the CdS was reduced to minimize its parasitic absorption property. The top and the bottom cell models were developed by using a special script introduced in SCAPS-1D solar cell capacitance simulator software. An artificial surface defect layer (SDL) was introduced between the window and the absorber of the top cell. The optimization procedure was carried out by altering the thicknesses of the top and the bottom absorbers and also varying the defect concentrations of the CdS/SDL interface and SDL/CdTe interface. The current matching condition of the tandem device and the device performance under the AM1.5G spectrum were also investigated. As the outcomes, we have identified the minimum possible defect density concentrations required for the window to absorber interfaces of the top cell to achieve the optimum performance. The experimental research work is suggested to further confirm the modeling results of the tandem device structure.

KEYWORDS: *Thin-film, Tandem, Surface Defect Layer, Defect Density, Bandgap, SCAPS-1D*

Corresponding author: Attygalle M.L.C., Email: lattygalle@sci.sjp.ac.lk

1 INTRODUCTION

CdTe is one of the most popular and ambitious semiconductor materials in the thin-film photovoltaics industry. It has been shown that the efficiency of this cell structure can be improved by up to 21% with 0.8759 V open-circuit voltage and 30.25 mA/cm^2 short circuit current (Green 2017) in a single cell model. CdS material was considered as a good buffer layer material and used with CdTe solar cells for a long time. But due to the parasitic absorption of CdS, many kinds of research were conducted to replace/reduce the material. In some cases CdS was removed and allowed the window layer to make direct contact with the absorber layer or the HRT layer was introduced with the buffer (Kephart et al. 2016).

Over the years, researchers have paid more attention to multijunction devices to improve the overall performances of the solar cells. According to the manuscript written by De. Vos (De Vos 1980) it was proven that the tandem cell can exceed the detailed balance limit of the single junction cell (Shockley & Queisser 1961). Since then, many types of research were conducted to discover the best efficient tandem model (Enam et al. 2017; Gupta & Dixit 2018; Wang 2019).

In this paper, we have considered a tandem cell with CdS/CdTe top cell and Si bottom cell with several modifications to improve the overall performance. The top cell was created with a transparent conducting oxide (TCO) layer, Mg-doped ZnO-based HRT layer (Bittau et al. 2017), buffer layer, the absorber layer, and back surface reflector layer (BSR) (Ratnasinghe & Attygalle 2019). This research work was conducted to optimize the tandem model and identify the range of minimum possible surface defect concentration levels of the CdS/CdTe interface (Attygalle & Ratnasinghe 2019). Also, the CdS buffer layer thickness was reduced to minimize parasitic absorption. A homojunction was created at the interface of the CdS/CdTe by considering the interface defects, and this layer was introduced as a surface defect layer.

The one-dimensional solar cell capacitance simulator (SCAPS-1D) software, which is developed under the supervision of Prof. Marc Burgelman, was used to model and simulate the tandem photovoltaic device (Niemegeers et al. 2014).

2 MATERIALS AND METHODS

2.1 Modeling Photovoltaic Device

The numerical modeling process was carried out by using the SCAPS-1D software which is developed at the Department of Electronics and Information Systems (ELIS) of the University of Ghent. Here, modified CdTe baseline model (Enam et al. 2017) was used as the top cell and a Si baseline model was used as the bottom cell. The top cell of the model is supposed to absorb high energy photons from the spectrum. Therefore, the materials with high energy bandgaps were used in the top cell model. The bandgaps of MZO (Sukauskas 2011), CdS, and CdTe were 3.7 eV, 2.4 eV, and 1.5 eV respectively.

In the top cell configuration, the SnO_2 layer is acting as a transparent conducting oxide (TCO). The HRT layer was considered as ZnO-based material (MZO) (Bittau et al. 2017) which has a higher energy bandgap, >3.3 eV (Bittau et al. 2018) and it creates flatter conduction band alignment with CdS. Due to the high optical transparency and wide-bandgap of the MZO layer, it was created between the SnO_2 and CdS layers. This will also make the benefit of reducing the optical losses at the window layer (Calnan 2014).

The SDL was created at the CdS/CdTe interface and this layer creates a homojunction with the CdTe absorber. This allows band bending at the SDL/CdTe interface. Therefore, low recombinations were expected at this point. The BSR was created with a heavily doped CdTe layer to reduce the recombinations at the back contact (Fossum & Burgess 1978; Von Roos 1978). The complete cell diagram is shown in Figure 1.

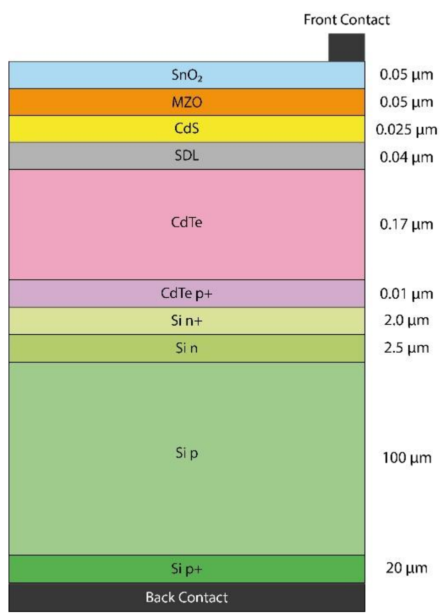

Figure 1: Complete architecture of the modeled tandem device structure

The bottom cell was created with c-Si to harvest the long-range wavelengths. These two cell structures were modeled separately due to the limitations of the SCAPS-1D software. The simulation part was carried out by combining these two cell models by using a SCAPS script.

In the combining method, we had to use two artificial layers to represent the top and bottom cells. Otherwise, the software will not recognize the partial absorption and partial reflection of the solar spectrum in tandem simulation. Therefore, the top cell was created with the artificial bottom layer and the bottom cell was created with an artificial top layer accordingly. These artificial layers have the thickness of modeled top and bottom cells (Figure 2). This is a unique technique used in the

SCAPS script simulations for tandem operations.

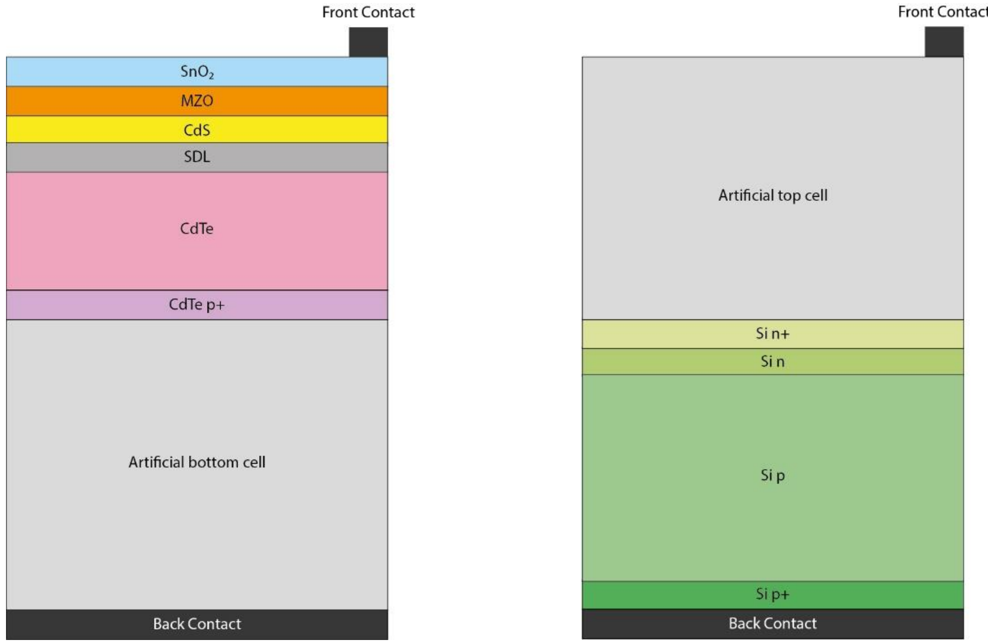

Figure 2: Separated top and bottom cell structures with artificial layers

2.2 Simulation

The two models were loaded into the script of the SCAPS-1D software and simulated under the AM1.5G spectrum (Bird et al. 1983) (under one sun illumination) with 1000 W/m^2 light power and a range of 300 – 1200 nm. Neither spectrum cutting off techniques nor neutral-density filters were used. The transmission was considered 100%. Here the simulation was repeated several times by altering the defect concentration levels of the interfaces of SDL and the thickness of the absorber of the top cell to obtain the optimum conditions.

The SCAPS software was programmed to perform mathematical functions such as the Poisson equation, continuity equation, and transport equation for electrons and holes. The Gummel iteration and Newton Raphson method are used to get the accurate condition by considering the convergence of the function.

The Shockley-Read-Hall recombination mechanism was used to simulate the recombinations via the intermediate defects states. Here, the radiative and auger recombination mechanisms were not considered.

The carrier density of the SDL and the defect density of the CdS/SDL and SDL/CdTe interfaces of the top cell were varied (Touafek & Mahamdi 2014) to observe the alterations of overall efficiencies of the tandem model. Meanwhile, the thicknesses of the top cell and bottom cell absorber layers were varied to optimize the tandem cell performance.

3 RESULTS & DISCUSSION

3.1 Influence of defect concentration of CdS/SDL and SDL/CdTe interfaces

According to our results, the SDL plays an important role in cell operation. The SDL compensates the homojunction with the absorber layer. In this study, this layer was introduced between the buffer layer and absorber to analyze its contribution. These defect densities of the interfaces were altered and identified the best configuration (Touafek & Mahamdi 2014).

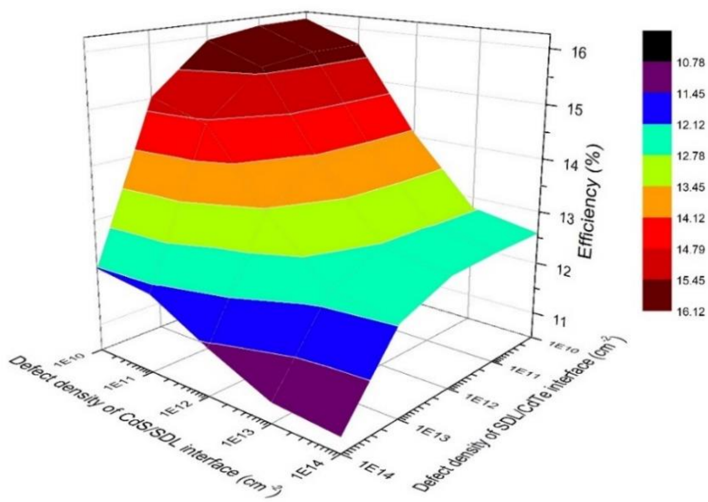

Figure 3: Defect density alteration of CdS/SDL and SDL/CdTe interfaces

Figure 3 shows the performance of the top cell (the efficiency variation) with the alteration of defect concentrations of the CdS/SDL and SDL/CdTe interfaces. The capture cross-section of CdS/SDL interface was considered as $\sigma n/p = 1\times10^{-15}$ cm^2. The bulk defect density of the SDL (n-CdTe) was considered as 1×10^{12} cm^{-3} (Song 2017). The interface defect concentration was altered between 1×10^{10} cm^{-2} and 1×10^{14} cm^{-2} and the maximum possible defect density at the CdS/SDL interface was identified as 1×10^{11} cm^{-2}. Increasing the defect density beyond this point will allow higher recombinations and it decreases the cell performance drastically. Similarly, the maximum possible defect density at the SDL/CdTe interface was identified as 1×10^{12} cm^{-2}.

3.1 Influence of the layer thicknesses and optimization

The thickness optimization of the top cell and bottom cell was also carried out by altering the thickness of CdTe and Si absorber layers respectively. The thickness of the SDL layer was considered as 0.04 µm. Increasing the thickness of the SDL enhanced the top cell performance but after a certain point, it weakened (Ouédraogo et al. 2014). The thickness of the CdTe layer of the top cell was altered between 0.1 – 0.18 µm. The efficiency of the top cell can be enhanced by increasing the thickness of the top cell (***Figure* 4**). The decrement of the open-circuit voltage (V_{OC}) was infinitesimal when compared to the change of short circuit current (J_{sc}). According to the tandem cell theory, increment of the top cell thickness will cause the gradual decrement of the efficiency of the bottom cell.

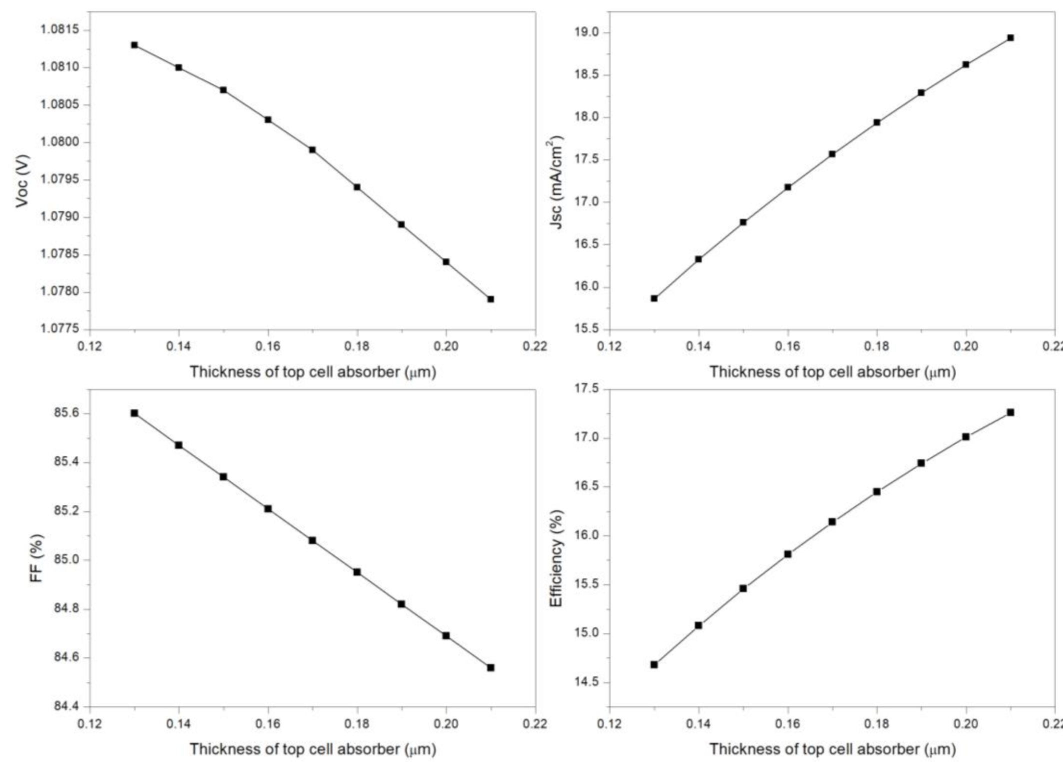

Figure 4: V_{oc} (Left-Top), J_{sc} (Right-Top), Fill Factor (Left-Bottom), Efficiency (Right-Bottom) of the top cell varying with the thickness of the top cell absorber

Figure 5 shows the decrement of the bottom cell performance with the increasing top cell thickness. Here the x-axis indicates the overall thickness of the top cell model. The top cell absorbs the high-energy photons of the AM1.5G solar spectrum with the average wavelength range of 300 nm to 850 nm. Increasing the thickness of the top cell causes higher absorption at the top cell and less amount of photons will penetrate to the bottom cell. The bottom cell optimization was carried out by varying the thickness of the Si absorber layer. Observed results show that the thickness of the absorber layer has a minor contribution to the tandem cell performance. Figure 6 represents the variation of bottom cell performance for different thickness values. The thickness was altered from 80 µm to 120 µm. At 100 µm, the bottom cell showed its peak performance of 8.65% efficiency with 0.59 V open-circuit voltage and 17.47 mA/cm^2 short circuit current density. At this point, the optimum length of the optical path was considered 100 µm for the maximum performance.This simulation was conducted for a certain thickness (0.31 µm) of the artificial top layer. The efficiency of the bottom cell can be varied with the artificial cell thickness, but in each case, the peak performance should appear for the optimum thickness value of the absorber layer.

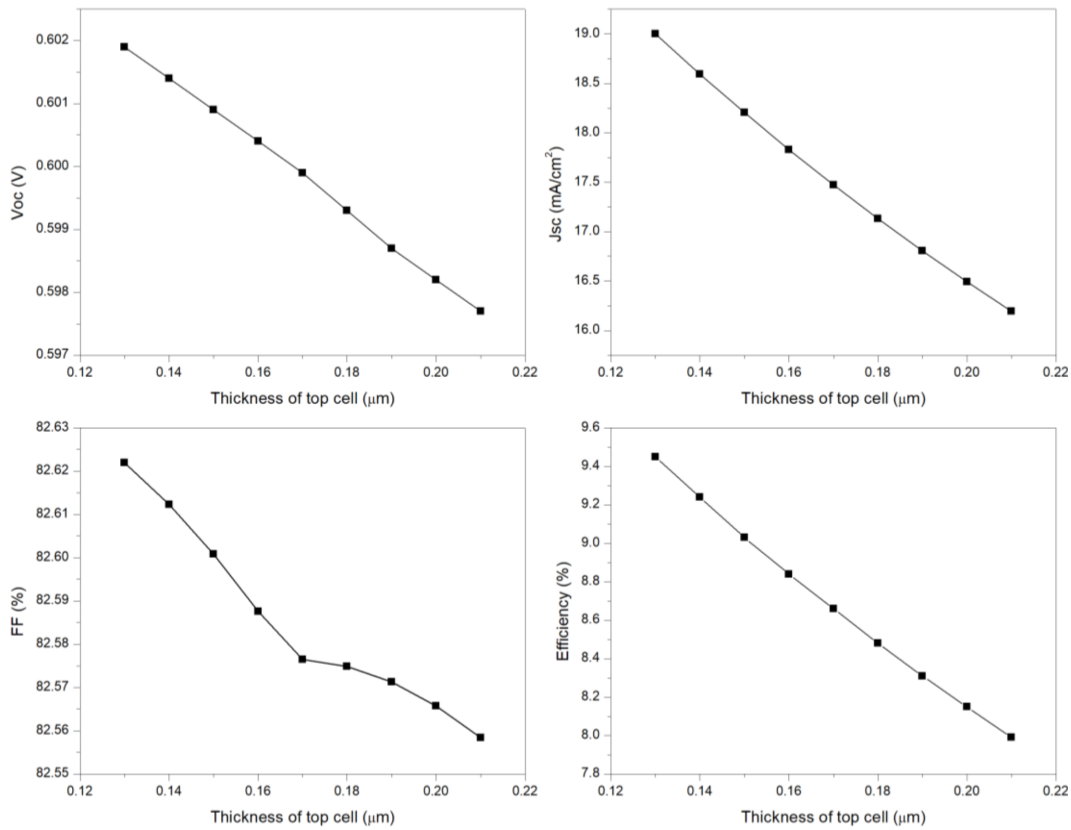

Figure 5: V_{oc} (Left-Top), J_{sc} (Right-Top), Fill Factor (Left-Bottom), Efficiency (Right-Bottom) of the bottom cell varying with the thickness of the top cell absorber

At the optimum point, the short circuit current of the top cell was matched with the short circuit current of the bottom cell. As shown in Figure 7, two linear curves intersect at 0.17 µm. Similarly, at the optimum absorber thickness of 0.17 µm, the overall efficiency of the tandem cell shows its peak performance.

The J-V characteristic curve demonstrates the current matching condition (Adewoyin et al. 2019) of the tandem cell and each open-circuit voltage. The open-circuit voltage (1.677 V) of the tandem cell was nearly equal to the summation of the open-circuit voltages of the top (1.078 V) and bottom (0.599 V) cells. It confirms that the two models are successfully working in tandem operation.

The EQE curve in Figure 8 represents the ratio between the number of carriers generated by the cell to the number of photons incidents for each top bottom and tandem models. Here the tandem curve was generated by calculating the summation of the values of each top and bottom cells. According to the observed results, the top and bottom cells show their peak performance in the wavelength ranges of 300-825 nm and 800-1000 nm respectively.

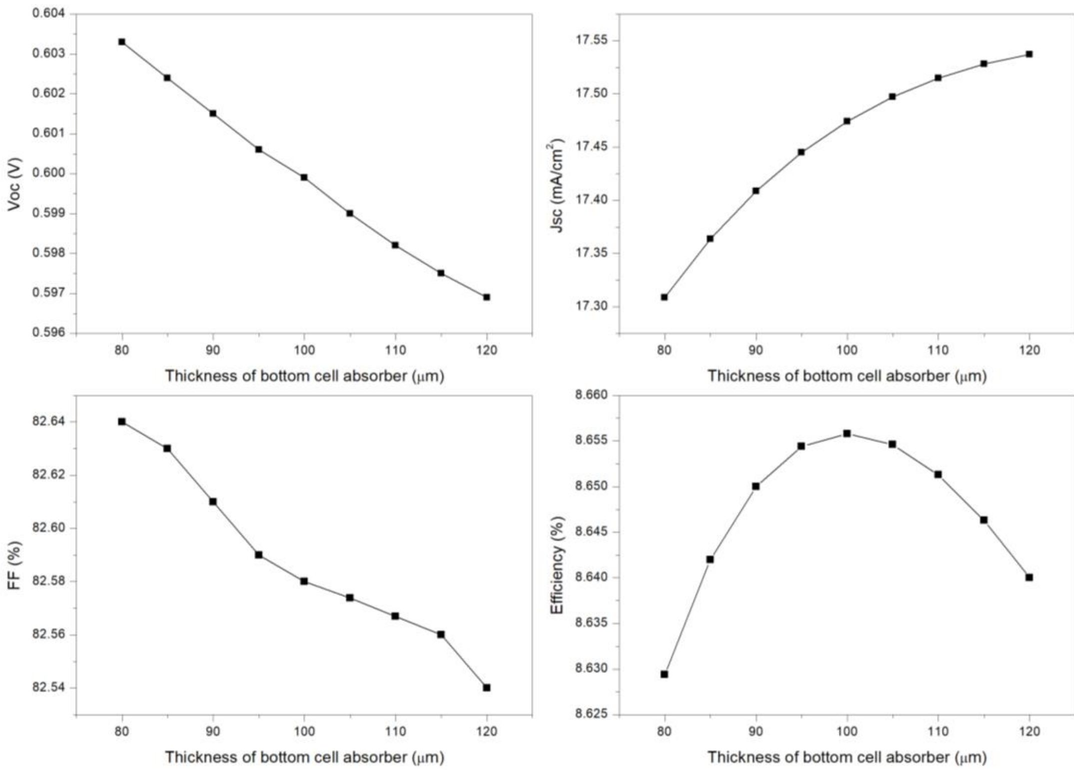

Figure 6: Parameter variation of the bottom cell thickness optimization

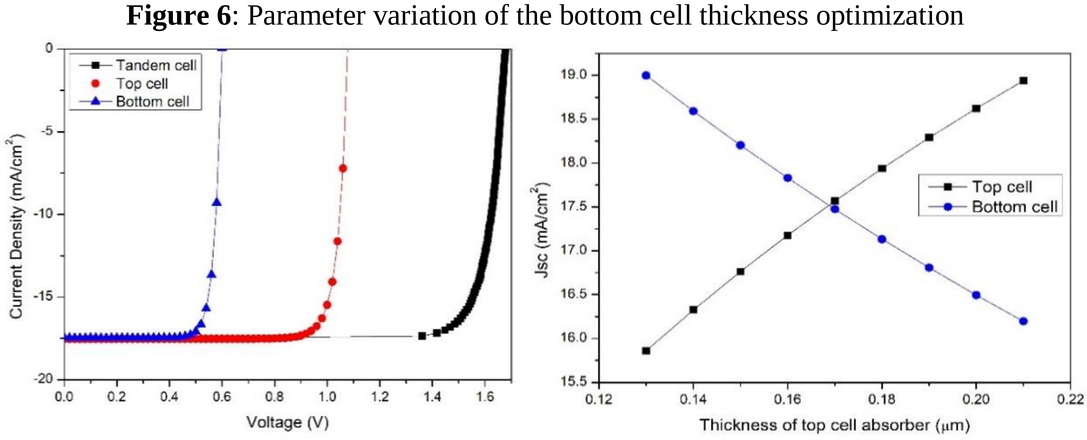

(a) (b)

Figure 7: Observed current matching condition closer to 0.17 µm (a) and J-V characteristic curves at current matching (b).

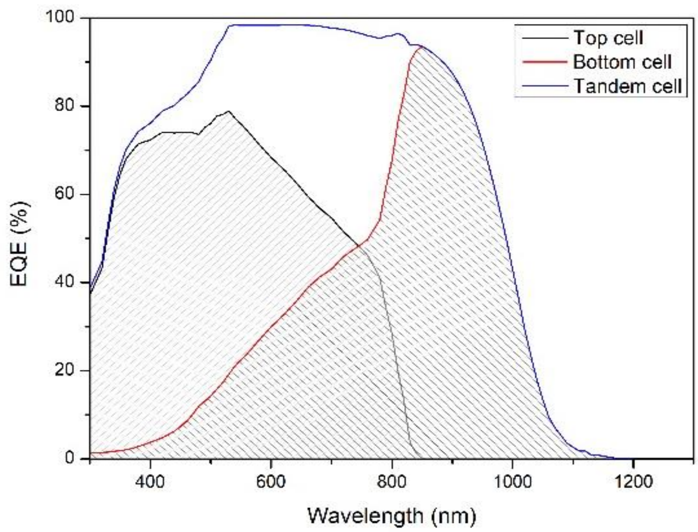

Figure 8: EQE curves of the top, bottom, and tandem cell structures

4 CONCLUSIONS

The three tasks of this simulation work were successfully completed. The defect density of the buffer/SDL interface should not exceed 1×10^{11} cm^{-2} and the SDL/absorber interface should not exceed 1×10^{12} cm^{-2} to gain the optimum efficiency of the device. The results confirm the maximum efficiency present at the lower defect densities at the interfaces. Specifically low defect density at buffer/SDL interface.

The bandgap of the surface defect layer should be the least possible value (1.5 eV) considering the bandgaps of the buffer and absorber layers. Increasing the defect density beyond 1×10^{10} cm^{-2} (CdS/SDL) and 1×10^{11} cm^{-2} (SDL/CdTe) will cause a drastic decrement in cell performance. In the optimization of both cell models, the short circuit currents were matched (17.47 mA/cm^2) at the optimum point of the tandem condition.

The tandem model with these surface defect concentrations showed a huge improvement when compared with the baseline model of the CdS/CdTe device which has a 0.87 V open-circuit voltage and 16.04% efficiency. Here efficiency of 24.72% was obtained with the tandem operation.

Adding an MZO layer with CdS makes a high influence on the tandem cell performance. The high optical transparency and the wide bandgap of this material play a major role in cell operation. The low thickness of the CdS layer with MZO was able to reduce the parasitic absorption in the 300-500 nm range.

According to the observed results, it has been shown that the performance of the tandem cell is strongly influenced by the thickness of the top cell absorber. The optimum thickness for the top cell and the bottom cell absorber materials were identified as 0.17 µm and 100 µm respectively. With these configurations, the tandem device with CdTe top cell and Si bottom cell show its peak performance. We would further suggest some experimental work to study the defects and the properties of the interfaces between window to absorber layer of the top cell to confirm the modeling results.

ACKNOWLEDGMENTS

All the authors gratefully acknowledge the "University of Sri Jayewardenepura" and the Ministry of the Science, Technology, and Research, Sri Lanka, for funding this project under the research grants ASP/01/RE/SCI/2016/29 and MSTR/TRD/AGR/03/02/15 respectively. Also, we would deeply acknowledge the helpful discussions and the ideas given by Prof. Marc Burgelman about modeling the tandem structures using SCAPS-1D.

REFERENCES

Adewoyin, AD, Olopade, MA, Oyebola, OO & Chendo, MA 2019. Development of CZTGS/CZTS tandem thin film solar cell using SCAPS-1D. *Optik*, 176, pp. 132-142.

Attygalle, M & Ratnasinghe, D 2019. Modelling of CdTe/Si Tandem Solar Cell With a Magnesium Doped Zinc Oxide Window Layer and Introducing a Surface Defects Layer Between Emitter/Absorber. *Proceedings of the 6th International Conference on Multidisciplinary Approaches (iCMA)*.

Bird, RE, Hulstrom, RL & Lewis, L 1983. Terrestrial solar spectral data sets. *Solar energy*, vol. 30, no. 6, pp. 563-573. doi:https://doi.org/10.1016/0038-092X(83)90068-3

Bittau, F, Artegiani, E, Abbas, A, Menossi, D, Romeo, A, Bowers, JW & Walls, JM 2017. Magnesium-doped zinc oxide as a high resistance transparent layer for thin film CdS/CdTe solar cells. *2017 IEEE 44th Photovoltaic Specialist Conference (PVSC)*. IEEE, pp. 752-756.

Bittau, F, Potamialis, C, Togay, M, Abbas, A, Isherwood, PJ, Bowers, JW & Walls, JM 2018. Analysis and optimisation of the glass/TCO/MZO stack for thin film CdTe solar cells. *Solar Energy Materials and Solar Cells*, 187, pp. 15-22.

Calnan, S 2014. Applications of oxide coatings in photovoltaic devices. *Coatings*, vol. 4, no.1, pp. 162-202. doi:10.3390/coatings4010162

De Vos, A 1980. Detailed balance limit of the efficiency of tandem solar cells. *Journal of Physics D: Applied Physics*, vol. 13, no. 5, p. 839. doi:https://doi.org/10.1088/0022-3727/13/5/018

Enam, FMT, Rahman, KS, Kamaruzzaman, MI, Sobayel, K, Bais, B, Akhtaruzzaman, M, Alamoud, ARM & Amin, N 2017. Design Prospects of Cadmium Telluride/Silicon (CdTe/Si) Tandem Solar Cells from Numerical Simulation. *Optik - International Journal for Light and Electron Optics*. doi:10.1016/j.ijleo.2017.03.106

Fossum, J & Burgess, E 1978. High-efficiency p+-n-n+ back-surface-field silicon solar cells. *Applied Physics Letters*, vol.33, no.3, pp. 238-240.

Green, MA 2017. Corrigendum to 'Solar cell efficiency tables (version 49)'[Prog. Photovolt: Res. Appl. 2017; 25: 3–13]. *Progress in Photovoltaics: Research and Applications,* vol. 25, no. 4, pp. 333-334.

Gupta, GK & Dixit, A 2018. Simulation studies of CZT (S, Se) single and tandem junction solar cells towards possibilities for higher efficiencies up to 22%. *arXiv preprint arXiv:1801.08498*.

Kephart, J, McCamy, J, Ma, Z, Ganjoo, A, Alamgir, F & Sampath, W 2016. Band alignment of front contact layers for high-efficiency CdTe solar cells. *Solar Energy Materials and Solar Cells,* 157, pp. 266-275.

Niemegeers, A, Burgelman, M, Decock, K, Verschraegen, J & Degrave, S 2014. SCAPS manual. *University of Gent*, pp. 65-92.

Ouédraogo, S, Zougmoré, F & Ndjaka, J 2014. Computational analysis of the effect of the surface defect layer (SDL) properties on Cu (In, Ga) Se2-based solar cell performances. *Journal of Physics and Chemistry of Solids,* vol. 75, no.5, pp. 688-695. doi:https://doi.org/10.1016/j.jpcs.2014.01.010

Ratnasinghe, D & Attygalle, M 2019. Numerical Investigation of the Best Efficient Tandem Solar Cell Structures Using the Base Cell Models of MZO/CdTe and CdS/CIGS Cell Structures. *IJMS,* vol.6, no.1, pp. 20-24. doi:http://doi.org/10.4038/ijms.v6i1.88

Shockley, W & Queisser, HJ 1961. Detailed balance limit of efficiency of p-n junction solar cells. *Journal of applied physics,* vol. 32, no. 3, pp. 510-519. doi:https://doi.org/10.1063/1.1736034

Song, T 2017. Design strategies for high-efficiency CdTe solar cells. *2000-2019-CSU Theses and Dissertations*.

Sukauskas, V 2011. Characterization of MgZnO epitaxial layers with high Mg concentration. In.

Touafek, N. & Mahamdi, R. 2014. Excess defects at the CdS/CIGS interface solar cells. *Chalcogenide Letters,* vol. 11, no. 11, pp. 589-596.

Von Roos, O 1978. A simple theory of back surface field (BSF) solar cells. *Journal of Applied Physics,* vol. 49, no. 6, pp. 3503-3511.

Wang, Y 2019. *Investigation of perovskite-CIGSe tandem solar cells.* Technische Universitaet Berlin (Germany).